A Pyrolysis Furnace with Reactor Tubes of Elliptical Cross Section

ARTICLE *in* INDUSTRIAL & ENGINEERING CHEMISTRY RESEARCH · JULY 1996

Impact Factor: 2.59 · DOI: 10.1021/ie9504009

2 AUTHORS:

Geraldine J. Heynderickx
Ghent University
98 PUBLICATIONS **983** CITATIONS
SEE PROFILE

Gilbert F. Froment
Texas A&M University
85 PUBLICATIONS **4,100** CITATIONS
SEE PROFILE

Article

A Pyrolysis Furnace with Reactor Tubes of Elliptical Cross Section

Geraldine J. Heynderickx, and Gilbert F. Froment

Ind. Eng. Chem. Res., **1996**, 35 (7), 2183-2189 • DOI: 10.1021/ie9504009

A Pyrolysis Furnace with Reactor Tubes of Elliptical Cross Section

Geraldine J. Heynderickx* and Gilbert F. Froment

Laboratorium voor Petrochemische Techniek, Universiteit Gent, Krijgslaan 281, B9000 Gent, Belgium

Circular tubes suspended in pyrolysis furnaces suffer from significant nonuniformities in heat flux, tube skin temperature, and coking rate profiles around the tube perimeter, due to the presence of "front" sides and "shadow" sides on the tubes. Simulation results for an ethane cracker with cracking tubes of elliptical cross section reveal that smoother circumferential heat flux, tube skin temperature, and coking rate profiles are obtained as the eccentricity of the elliptical tubes increases. The circumferential maximal values in coking rates are reduced by 30%. The more uniform tube skin temperature distributions and coke layers in tubes of elliptical cross section favor the run length of the furnace and the tube metal life.

Introduction

Thermal cracking of hydrocarbons to olefins is an endothermal process. The reactor coils, in which the thermal cracking reactions take place, are suspended in large, gas-fired furnaces. Over 90% of the heat transfer from the furnace to the reactor coils is due to radiation. Radiative heat transfer requires heat source and heat sink to "see" one another. The calculation of circumferential tube skin temperature profiles in thermal cracking coils (Heynderickx et al., 1992) revealed significant nonuniformities in heat flux, temperature, and coking rate profiles around the tube perimeter. Tubes have two "front" sides and two "shadow" sides. The lowest temperatures were calculated in the plane of the tube row, and the highest temperatures, on the tube zones directly facing the furnace walls.

In the present paper, the use of reactor tubes with elliptical cross section, as an alternative for the cylindrical thermal cracking tubes, is investigated. Suspending the elliptical tubes in the furnace with the major axis parallel to the tube row increases the front side and decreases the shadow side on the tubes.

This paper presents simulation results for a single-row ethane cracker with elliptical tubes of different sizes, obtained with the CRACKSIM and FURNACE simulation programs developed at the Laboratory for Petrochemical Engineering (University of Ghent, Belgium). The results are compared with previously obtained results for the same furnace with cylindrical tubes (Heynderickx et al., 1992).

Model Equations and Simulation Procedure

Reactor Model. The set of continuity equations for the various species is solved simultaneously with the energy equation and the pressure drop equation (Froment and Bischoff, 1990):

$$\frac{\mathrm{d}F_j}{\mathrm{d}z} = (\sum_i n_{ij} r_{ri}) \frac{\pi d_t^{\,2}}{4} \tag{1}$$

$$\sum_j F_j c_{pj} \frac{\mathrm{d}T}{\mathrm{d}z} = Q(z)\,\pi d_t + \frac{\pi d_t^{\,2}}{4} \sum_i r_{ri} (-\Delta H)_i \tag{2}$$

$$\left(\frac{1}{M_m p_t} - \frac{p_t}{\alpha G^2 R T}\right) \frac{\mathrm{d}p_t}{\mathrm{d}z} = \frac{\mathrm{d}}{\mathrm{d}z}\left(\frac{1}{M_m}\right) + \frac{1}{M_m}\left(\frac{1}{T}\frac{\mathrm{d}T}{\mathrm{d}z} + Fr\right) \tag{3}$$

with

$$Fr = 0.092 \frac{Re^{-0.2}}{d_t} \tag{4}$$

for the straight parts of the reactor coils and

$$Fr = 0.092 \frac{Re^{-0.2}}{d_t} + \frac{\zeta}{\pi R_b} \tag{5}$$

for the tube bends, with

$$\zeta = \left(0.7 + 0.35 \frac{\Lambda}{90°}\right)\left(0.051 + 0.19 \frac{d_t}{R_b}\right) \tag{6}$$

For the tubes of elliptical cross section, the tube diameter d_t is replaced by the equivalent tube diameter d_e:

$$d_e = 4\frac{S}{O} \tag{7}$$

A detailed radical reaction scheme is combined with a one-dimensional plug flow model to simulate the cracking reactions in the reactor coil. Reynolds numbers on the order of 250 000 are calculated in the reactor tubes. The turbulence wipes out temperature profiles in the process gas over the cross section of the reactor tubes.

The kinetic scheme is based on a complete reaction network for the decomposition of the ethane feed. The reaction network contains 1054 reactions: 56 initiation reactions, 572 H-abstractions, 126 radical additions, 126 decomposition reactions, 6 isomerization reactions, 56 termination reactions and a number of molecular Diels−Alder cyclizations (Willems and Froment, 1988a,b).

Furnace Model. The furnace model is based upon the zone method of Hottel and Sarofim (1967). The furnace wall, the tube skin, and the flue gas volume are divided into a number of isothermal elements with uniform properties. For each of these elements, named zones, the energy balance is set up, taking into account the contributions of convective, conductive, and radiative heat transfer. The contributions of radiative transfer are obtained through Monte Carlo simulation (Plehiers and Froment, 1989), calculating the view factors be-

* Author to whom correspondence should be addressed. E-mail address: gh@elptrs1.rug.ac.be.

S0888-5885(95)00400-3 CCC: $12.00

tween the different zones in the furnace. From these view factors, the total exchange area Z_iZ_j between the zones Z_i and Z_j in the furnace is determined. The total exchange area Z_iZ_j is the amount of radiative energy emitted by the zone Z_i in the direction of the zone Z_j, divided by the black body emissive power of the zone Z_i. The emissive power of a black body with temperature T_i is calculated from the Stefan−Boltzmann law:

$$E_i = \sigma T_i^4 \tag{8}$$

The determination of Z_iZ_j is discussed in detail by Rao et al. (1988) and by Plehiers and Froment (1989).

The set of energy balances for the furnace can be written as:

$$\begin{bmatrix} Z_1Z_1 - \sum_j Z_1Z_j & Z_2Z_1 & \dots & Z_nZ_1 \\ Z_1Z_2 & Z_2Z_2 - \sum_j Z_2Z_j & \dots & Z_nZ_2 \\ \vdots & \vdots & \vdots & \vdots \\ Z_1Z_n & Z_2Z_n & \dots & Z_nZ_n - \sum_j Z_nZ_j \end{bmatrix} \times \begin{bmatrix} E_1 \\ E_2 \\ \vdots \\ E_n \end{bmatrix} = \begin{bmatrix} Q_1A_1 \\ Q_2A_2 \\ \vdots \\ Q_nA_n \end{bmatrix} \tag{9}$$

where Q_i represents the nonradiative heat flux emitted by the zone Z_i with area A_i.

Solving this set of energy equations yields the heat flux and temperature profiles in the furnace. To calculate the circumferential temperature distribution in the tube wall, the tubes are discretized along the tube perimeter and over the tube skin. By constructing and solving the energy balance for each element in the tube skin, circumferential heat flux and temperature profiles are calculated in the tube skin. The form of these energy balances for the zones in the tube skin is discussed by Heynderickx et al. (1992). They are obtained by discretizing the conduction equation for each zone in the reactor tube skin, accounting for the appropriate boundary conditions:

$$\nabla^2 T = \frac{d^2T}{dr^2} + \frac{1}{r}\frac{dT}{dr} + \frac{1}{r^2}\frac{d^2T}{d\theta^2} = 0 \tag{10}$$

$$\lambda \nabla T(\theta,r) = q(\theta,r) \qquad r = r_{ext}; \quad \forall\theta$$

$$\lambda \nabla T(\theta,r) = h_p(T(\theta,r) - T_p) \qquad r = r_{int}; \quad \forall\theta$$

Simulation Procedure. A simplified flow chart of the iterative calculation scheme is given in Figure 1. The calculation was performed on a Data General MV15000. Five hours of CPU time is required to calculate the view factors for a given geometry of furnace and reactor coils. Starting from appropriate initial estimates for temperature and heat flux profiles in the furnace, an additional 3 h of CPU time is required for one simulation case to converge to its solution.

Furnace Description

The main dimensions and operating conditions of the ethane cracking furnace are summarized in Table 1.

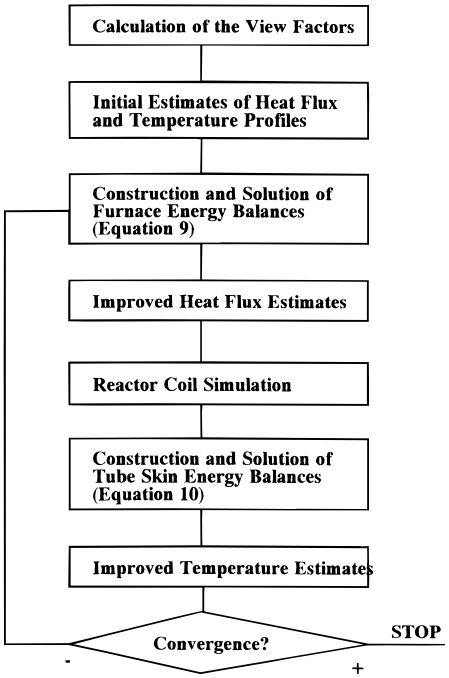

Figure 1. Flow diagram of the calculations.

Table 1. Furnace Dimensions and Operating Conditions

furnace	
length (mm)	4652
height (mm)	13 450
width (mm)	2100
thickness of refractory (mm)	230
thickness of insulation (mm)	50
no. of side wall burners	64
firing conditions	
total heat input	16.53 MW
operating conditions	
feedstock	100% ethane
hydrocarbon feed rate (kg/h/coil)	3657
steam dilution (kg/kg)	0.332
coil inlet temperature (°C)	660
coil outlet pressure (atm)	1.28
material properties	
emissivity of furnace wall	0.60
emissivity of tube skin	0.95
thermal conductivity of	
refractory (W/m K)	$0.0193 + 118.0 \times 10^{-6}T$ (K)
insulation (W/m K)	$0.0452 + 111.1 \times 10^{-6}T$ (K)
tube skin material (W/m K)	$-8.432 + 3.040 \times 10^{-2}T$ (K)

Two reactor coils, with eight passes each, are suspended in the furnace. The furnace is heated with 64 radiation burners positioned in eight rows of four burners in the front and in the rear wall of the furnace. Top and front views of the furnace are shown in Figures 2 and 3.

Four coupled furnace and reactor tube simulations with elliptical tubes of different dimensions were performed. The coupled simulation of the furnace with circular tubes was also performed.

The internal cross section of the different elliptical tubes was taken equal to that of the circular tube. This allows for identical hydrocarbon feed and steam rates to the reactor coils, simplifying comparison of the results for the different simulation cases. The external major axis of the different elliptical tubes was taken to exceed the external diameter of the circular tube by 10 (type 1), 20 (type 2), 30 (type 3), and 40% (type 4).

Finally, the tube pitch was the same for both types of tubes, in order to retain the furnace dimensions. The dimensions of the tubes with circular and elliptical cross

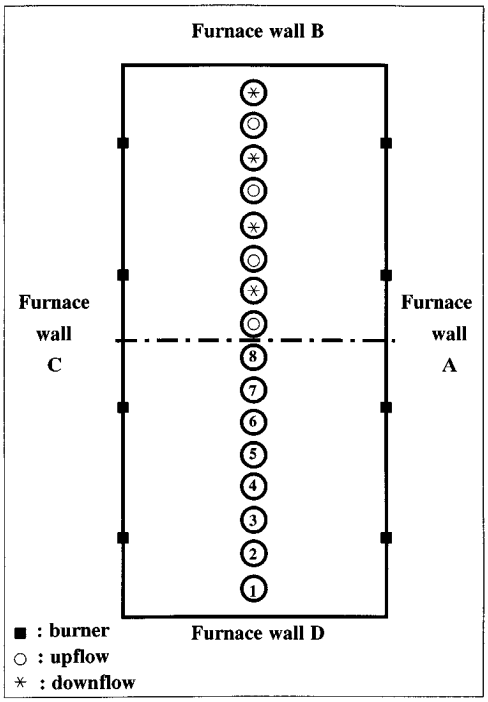

Figure 2. Top view of the ethane furnace.

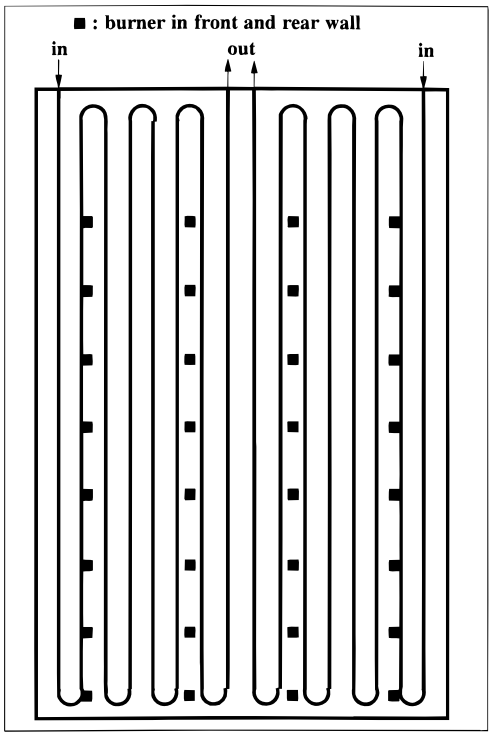

Figure 3. Front view of the ethane furnace.

section are compared in Table 2. The perimeters of the elliptical tubes were determined by numerical integration of the elliptical integral of the second kind:

$$P = 4a\int_0^{\pi/2}\left(1 - \left(1 - \frac{b^2}{a^2}\right)\sin^2\phi\right)^{1/2} \mathrm{d}\phi \qquad (11)$$

In this expression, ϕ represents the angle of the parameter equation of the ellipse (Figure 4)

$$x = a\sin\phi \qquad \text{and} \qquad y = b\cos\phi \qquad (12)$$

with a and b the semimajor and semiminor axes of the ellipse. For identical cross sections of the circular and the elliptical tubes, the perimeter of the elliptical tubes is larger than that of the circular tube. For the tubes considered in this paper, a maximum difference of 9% was calculated (Table 2).

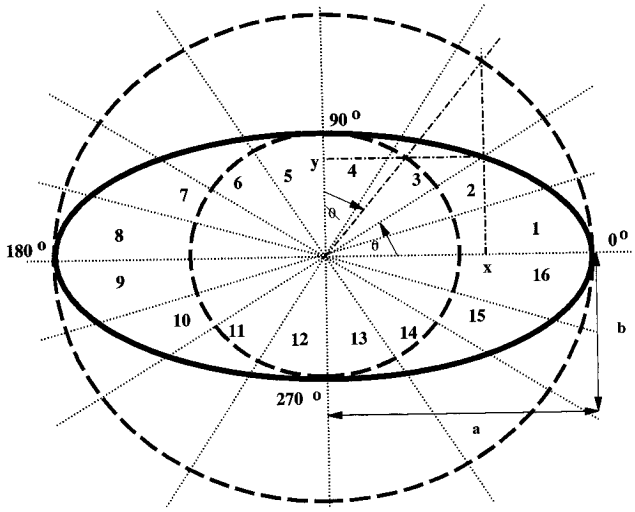

Figure 4. Circumferential division of the tube.

Table 2. Tube Dimensions

tube type	circular	elliptical			
major axis/diameter		1.1	1.2	1.3	1.4
eccentricity ϵ	0	0.56	0.71	0.80	0.86
total coil length (m)		102.336			
no. of passes		8			
internal cross section (m^2)					
passes 1−6		0.012076			
passes 7 and 8		0.014527			
wall thickness (mm)		8			
external diameter (mm)					
passes 1−6	140				
passes 7 and 8	152				
external major axis (mm)					
passes 1−6		154	168	182	196
passes 7 and 8		167	182	198	213
external minor axis (mm)					
passes 1−6		127	117	109	101
passes 7 and 8		138	127	118	110
external perimeter (mm)					
passes 1−6	439.8	443.0	451.6	463.8	479.1
passes 7 and 8	477.5	481.0	490.1	504.0	520.0

The furnace was divided into zones by means of four planes parallel to the furnace bottom plate. The five axial zones on the fourth, fifth, and sixth pass of the reactor coil through the furnace were circumferentially divided into 16 zones, as presented in Figure 4 for the ellipse with maximum eccentricity (elliptical tube of type 4).

For reasons of symmetry, only half a furnace has to be calculated, leading to a total of 162 zones in the furnace: 145 (external) tube skin zones, 12 furnace wall zones, and 5 flue gas volume zones.

Results and Discussion

The average cracking results obtained for the circular and elliptical tubes are compared in Table 3 and Figures 5−11.

The heat flux profiles along the reactor coil are presented in Figure 5. The average heat flux to the reactor tubes, for a total furnace heat input of 16.53 MW, drops by 6% from 85.5 kW/m_{ext}^2 for the circular tube to 80.5 kW/m_{ext}^2 for the elliptical tube of type 4. However, the perimeter of the elliptical tube of type 4

Table 3. Simulation Results

tube type	circular	elliptical			
major axis/diameter		1.1	1.2	1.3	1.4
flue gas outlet T (°C)	1064	1060	1055	1049	1041
furnace efficiency (%)	47.6	47.8	48.1	48.4	48.8
max heat flux (kW/m_{ext}^2)	116	115	114	111	109
average heat flux (kW/m_{ext}^2)	85.5	85.2	84.2	82.4	80.5
coil outlet T (°C)	856	858	859	860	862
max tube skin T (°C)	979	978	977	974	972
ethane conversion (%)	66.3	66.6	67.1	67.7	68.4
ethylene yield (wt %)	52.1	52.2	52.5	52.8	53.1
max. coking rate (g/m^2 h)	29.5	29.4	29.0	27.8	27.2
residence time (ms)	596	597	598	600	603
pressure drop (atm)	1.93	1.95	1.97	2.00	2.02

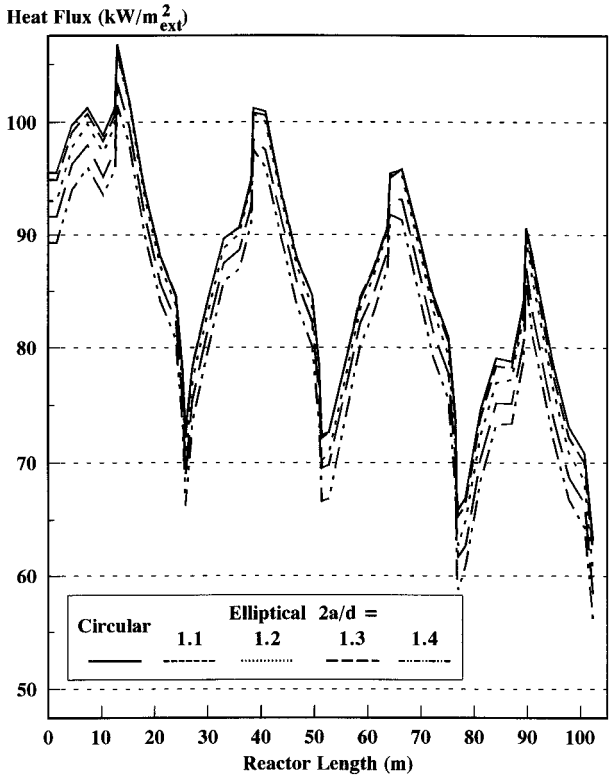

Figure 5. Heat flux profiles along the coil.

(479.1 and 520.0 mm) exceeds that of the circular tube (439.8 and 477.5 mm) by 9%. The combination of lower average heat flux and higher tube skin surface for the elliptical tubes leads to a higher total heat input in the elliptical tubes, resulting in a higher conversion of the ethane feed. It increases from 66.3% for the circular tube to 68.4% for the elliptical tube of type 4 (Figure 6). The ethylene yield rises from 52.08 wt % for the circular tube to 53.11 wt % for the elliptical tube of type 4, as shown in Figure 7. The (molar) ethylene selectivity drops by 1% from 0.84 to 0.83.

The efficiency of the heat transfer from furnace to reactor tube increases from 47.6% for the furnace with circular tubes to 48.8% for the furnace with elliptical tubes of type 4. The corresponding flue gas temperature profiles are shown in Figure 8. The flue gas outlet temperature drops by 23 °C from 1064 °C for the furnace with circular tubes to 1041 °C for the furnace with elliptical tubes of type 4.

The process gas and external tube skin temperature profiles are presented in Figures 9 and 10. The process outlet temperature increases from 858 °C for the circular tube to 862 °C for the elliptical tube of type 4. The maximum (*average*) tube skin temperature decreases from 979 to 972 °C, due to the lower heat fluxes to the elliptical reactor tubes.

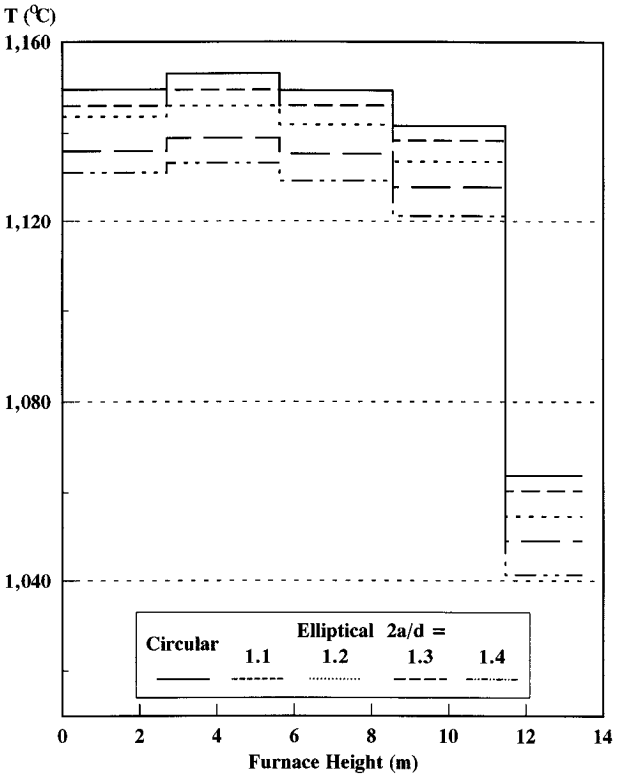

Figure 6. Flue gas temperature distribution.

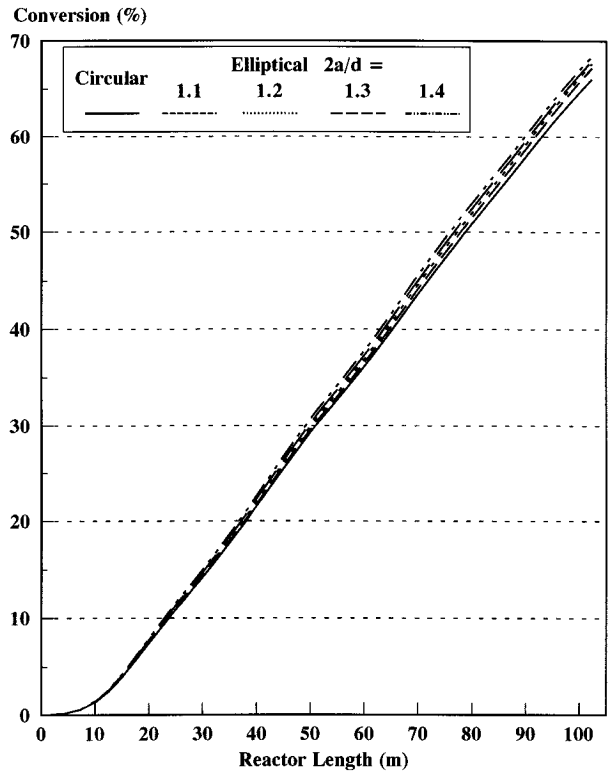

Figure 7. Conversion profiles.

The rate of coke formation in the various tubes is shown in Figure 11. As the eccentricity of the elliptical tubes increases, the average rate of coke formation decreases, due to the lower average tube skin temperatures. The average maximum coking rate drops from 29.4 to 27.2 g/m^2 h when the circular tube is replaced by an elliptical tube of type 4. The lower coking rate increases the run length of the furnace.

The pressure drop in the elliptical tubes is somewhat higher than that in the circular tubes.

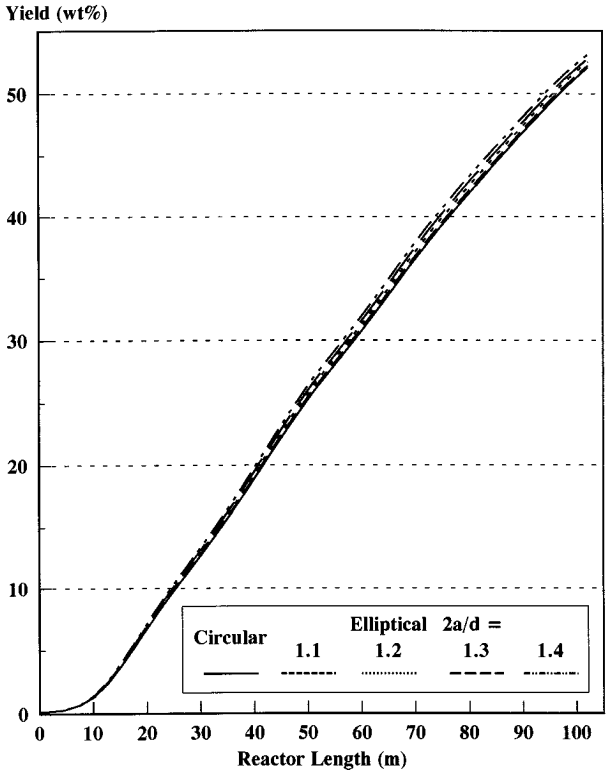

Figure 8. Ethylene yield profiles.

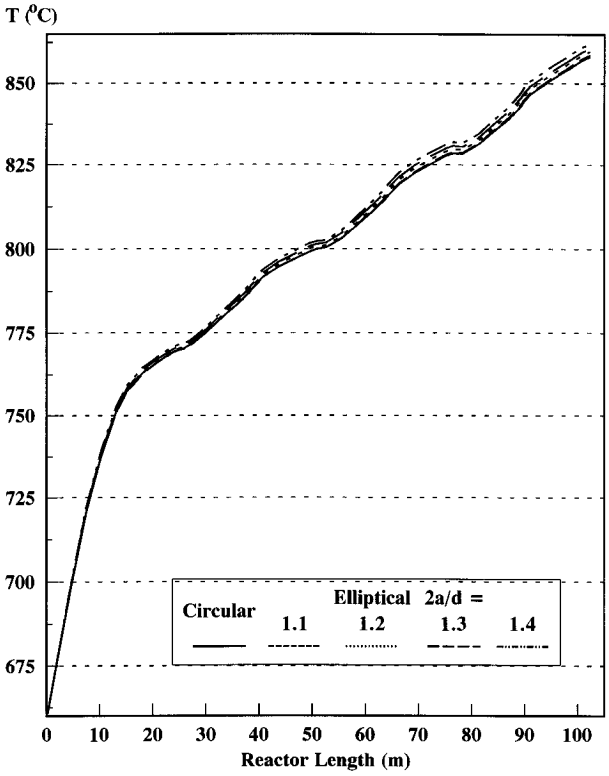

Figure 9. Process gas temperature profiles.

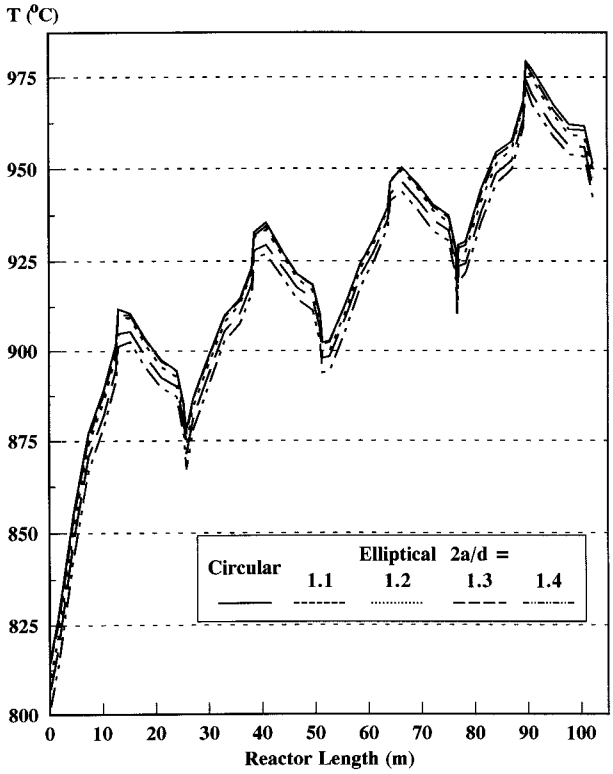

Figure 10. External wall temperature profiles.

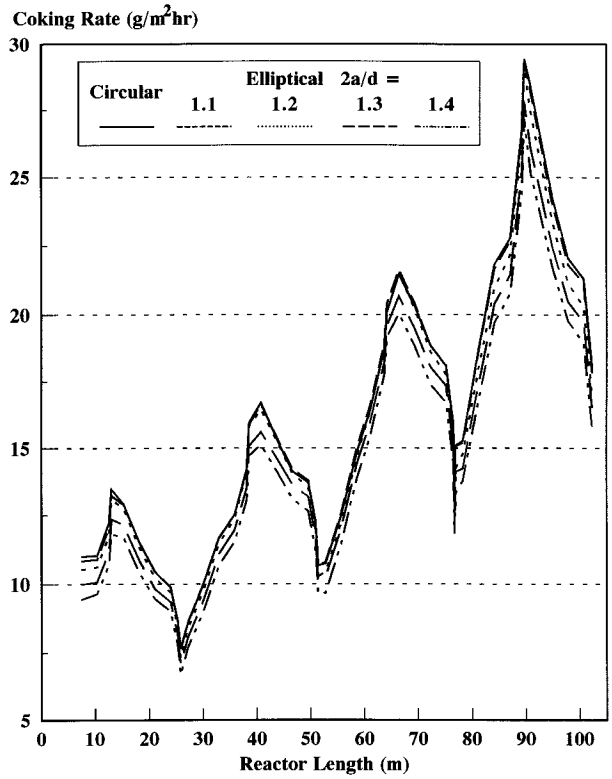

Figure 11. Coking rate profiles along the coil.

To obtain a similar process gas outlet pressure of 1.28 atm for all tube types, an initial process gas inlet pressure of 3.30 atm is required for the elliptical tube of type 4, while an initial inlet pressure of 3.22 atm meets the demand for the circular tube. However, due to the lower coking rates, the reactor tube inlet pressure for the elliptical tube will grow slower with time, compared to the circular tube.

The external tube skin temperature of thermal cracking coils is measured with radiation pyrometers. Heynderickx et al. (1992) showed that circumferential nonuniformities in temperature occur on the tube skin. The measured value, therefore, depends on the measuring spot on the tube perimeter. The local maximum temperature can easily exceed the average temperature by 20 °C. Elliptical tubes have a larger front side than circular tubes. Since the tube perimeter "sees" more of the front and rear walls of the furnace, it is expected that the nonuniformities in temperature and heat flux

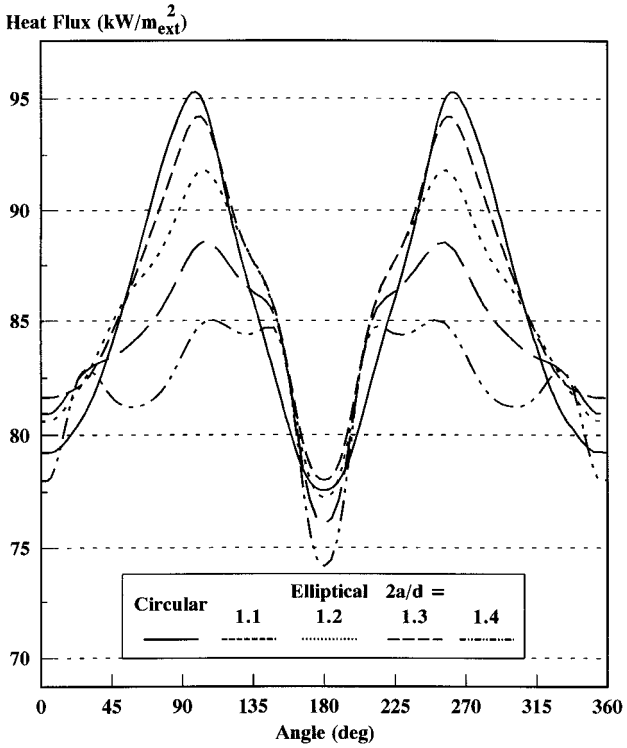

Figure 12. Circumferential heat flux profiles (tube 5; axial division 3).

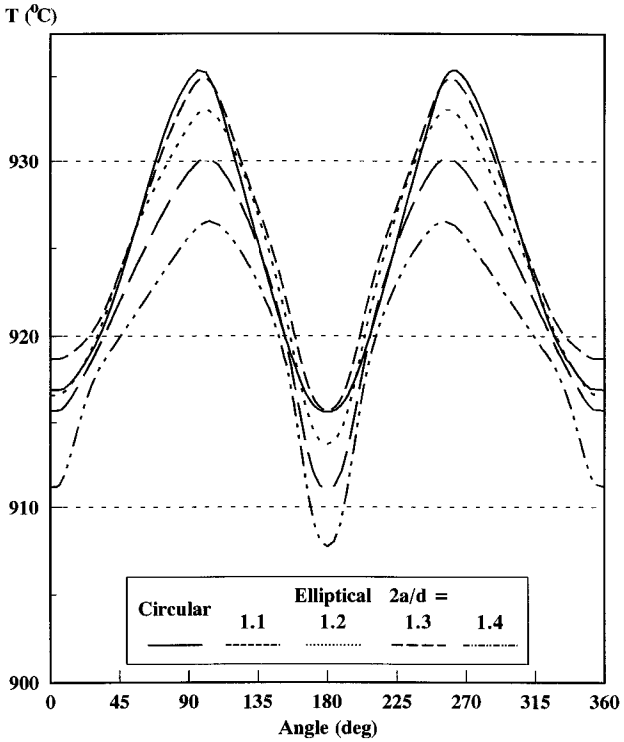

Figure 13. External circumferential tube skin temperature profiles (tube 5; axial division 3).

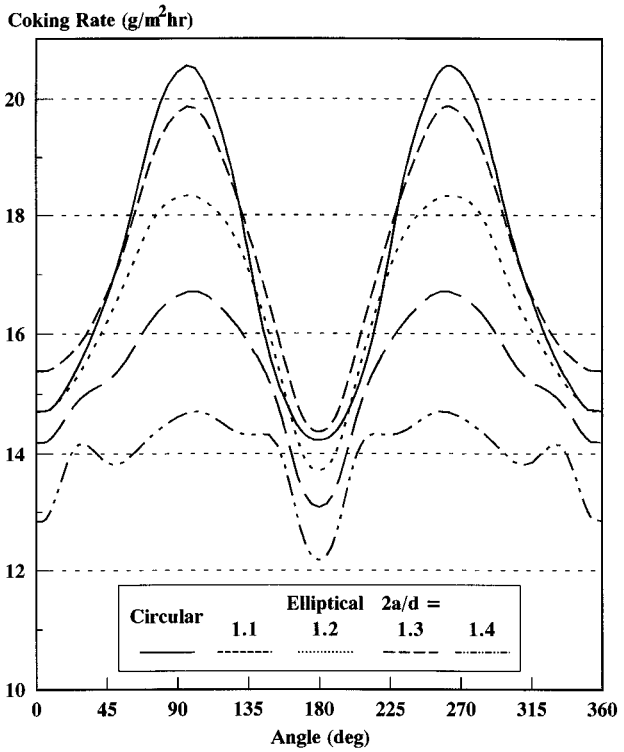

Figure 14. Circumferential coking rate profiles (tube 5; axial division 3).

decrease as the eccentricity of the ellipse increases. Calculated circumferential heat flux profiles for the different tube types are shown in Figure 12. These profiles were calculated at a reactor length of 57.5 m (third axial division on the fifth pass of the reactor coil through the furnace). For all tube types, maxima are calculated on the parts of the tubes directly facing the long furnace walls (90° and 270°); minima are calculated in the plane of the tubes (0° and 180°). The circumferential nonuniformities are seen to be gradually smoothened out as the eccentricity of the tubes increases. This is due to the increase of front side on the more eccentric tubes. Replacing the circular tube by an elliptical tube has almost no influence on the cold parts of the tubes, which are still shadowed by the neighboring tubes. The heat flux calculated at the circumferential position of 0° on the tube skin is somewhat higher than the value calculated at the 180° position. This is due to the position of the burners relative to the fifth tube, as can be seen from Figure 3. Also, the tube pitch was not changed, resulting in a smaller distance between the outer shells of two neighboring tubes as the tube eccentricity increases. An increase of the tube pitch might increase the temperature of the cold parts of the elliptical tubes. The external heat fluxes on the circular tube vary by over 20%. This variation is reduced to less than 9% for an elliptical tube of type 4. The total circumferential tube skin temperature variation remains almost constant for the different tube types: 21 °C for the circular tube and 19 °C for the elliptical tube of type 4 (Figure 13). If the shadow zones are not considered, the circumferential temperature variation for the elliptical tube of type 4 is not higher than 10 °C, while a variation of 17 °C is calculated for the circular tube. A more even temperature distribution around the tube skin is obtained for the elliptical tube.

Undesired side reactions in the thermal cracking process lead to the formation of a coke layer on the internal tube skin. The rate of coke formation is determined by the concentration of the coke precursors and (for a clean tube) by the internal tube skin temperature. A more uniform tube skin temperature profile results in a more uniform thickness of the coke layer. The calculated circumferential rate of coke formation is shown in Figure 14. For the circular tube, coking rate variations of nearly 50% between 14 and 20.5 g/m^2 h are calculated. For the elliptical tube of type 4, the coking rate varies between 12 and 14.5 g/m^2 h. If the shadow zones are not considered, an almost identical

coking rate of 14 g/m^2 h around the tube perimeter of the elliptical tube of type 4 is obtained; for the circular tube, the coking rate still varies by 20%. A more uniform and thinner coke layer is obtained with the elliptical tubes (especially of type 4) than with the circular tubes. This limits the increase in pressure drop with time for the elliptical tubes. The uniform circumferential tube skin temperature profiles for the elliptical tubes are retained, while the circumferential profiles for the circular tube become even more pronounced with time.

Conclusion

The average heat flux from furnace to reactor coil is lower for elliptical tubes than for circular tubes. Due to the low heat fluxes, lower tube skin temperatures are obtained, resulting in lower coking rates and a longer run length of the furnace with elliptical tubes.

More uniform heat flux and temperature conditions around the elliptical tube perimeter are obtained. The coke layer thickness around the elliptical tube perimeter is more even; the pressure drop over the reactor coil grows at a lower rate. In circular tubes, the circumferential profiles become more pronounced with time. This is less likely to occur in elliptical tubes.

For a tube of elliptical cross section, an additional investment in tube skin material is required to obtain the same conversion as in the corresponding circular tube. This investment amounts to no more than 6% for the elliptical tube of type 4, which gives completely uniform profiles on the front part of the tube.

Other factors still to be considered in the comparison between circular and elliptical tubes are the respective costs and the behavior under severe operating conditions.

Nomenclature

A_i: area of zone i (m^2)
a: semimajor axis of ellipse (m)
b: semiminor axis of ellipse (m)
c: center-to-focus distance of ellipse $(a^2 - b^2)^{0.5}$ (m)
c_p: heat capacity (J/mol K)
d_e: equivalent diameter of elliptical tube (m)
d_t: tube diameter (m)
E: black body emissive power (W/m^2)
F: molar flow rate (mol/h)
G: total mass flux of process gas (kg/m^2 s)
h_p: convection coefficient (W/m^2 K)
$-\Delta H$: heat of reaction (J/mol)
M_m: average molecular weight (kg/mol)
n: stoichiometric coefficient
O: wetted perimeter (m)
P: perimeter of ellipse (m)
p_t: total pressure (Pa)
Q: heat flux (W/m^2)
q: heat flux (W/m^2)
r: radius (m)
Re: Reynolds number
R_b: radius of tube bend (m)
r_r: reaction rate (mol/m^3 s)
S: wetted area (m^2)
s: tube pitch (m)
T: temperature (K)
z: axial reactor coordinate (m)
Z_iZ_j: total exchange area between zones i and j (m^2)

Greek Letters

α: unit conversion factor
ϵ: eccentricity of ellipse
θ: polar coordinates angle (Figure 4) (rad)
ϕ: angle in parameter equation of ellipse (Figure 4) (rad)
Λ: tube bend angle (deg)
σ: Stefan−Boltzmann constant (5.7×10^{-8} W/m^2 K^4)

Literature Cited

Froment, G. F.; Bischoff, K. B.*Chemical Reactor Analysis and Design*; John Wiley and Sons: New York, 1990.

Heynderickx, G. J.; Cornelis, G. G.; Froment, G. F. Circumferential Tube Skin Temperature Profiles in Thermal Cracking Coils. *AIChE J.* **1992**, *38*, 1905.

Hottel, H. C.; Sarofim, A. F. *Radiative Heat Transfer*; McGraw-Hill: New York, 1967.

Plehiers, P. M.; Froment, G. F. Firebox Simulation of Olefin Units. *Chem. Eng. Commun.* **1989**, *80*, 81.

Rao, M. V. R.; Plehiers, P. M.; Froment, G. F. Simulation of the Run Length of an Ethane Cracking Furnace. *Ind. Eng. Chem. Sci.* **1988**, *43*, 1223.

Willems, P.; Froment, G. F. Kinetic Modeling of the Thermal Cracking of Hydrocarbons, Part 1: Calculation of Frequency Factors. *Ind. Eng. Chem. Res.* **1988a**, *27*, 1959.

Willems, P.; Froment, G. F. Kinetic Modeling of the Thermal Cracking of Hydrocarbons, Part 2: Calculation of Activation Energy. *Ind. Eng. Chem. Res.* **1988b**, *27*, 1966.

Received for review July 3, 1995
Accepted March 11, 1996[⊗]

IE9504009

[⊗] Abstract published in *Advance ACS Abstracts,* June 1, 1996.